

Electromigration and thermomigration behavior of flip chip solder joints in high current density packages

D. Yang, Y.C. Chan,^{a)} and B.Y. Wu

Department of Electronic Engineering, City University of Hong Kong, Kowloon Tong, Hong Kong

M. Pecht

Center for Advanced Life Cycle Engineering (CALCE), University of Maryland, College Park, Maryland 20742

(Received 31 December 2007; accepted 11 March 2008)

The electromigration and thermomigration behavior of eutectic tin-lead flip chip solder joints, subjected to currents ranging from 1.6 to 2.0 A, at ambient temperatures above 100 °C, was experimentally and numerically studied. The temperature at the chip side was monitored using both a temperature coefficient of resistance method and a thermal infrared technique. The electron wind force and thermal gradient played the dominant role in accelerated atomic migration. The atomic flux of lead due to electromigration and thermomigration was estimated for comparison. At the current crowding region, electromigration induced a more serious void accumulation as compared with thermomigration. Also, because of different thermal dissipations, a morphological variation was detected at different cross-sectional planes of the solder joint during thermomigration.

I. INTRODUCTION

The pursuit of greater performance in microelectronic power devices has led to shrinkage of solder joint size and a significant increase in current. This has resulted in a dramatic increase in the current density passing through the solder joints and has placed challenges on product reliability. According to the 2006 International Technology Roadmap for Semiconductors (ITRS), electromigration in solder, defined as the solid-state atomic movement because of momentum transfer from flowing electrons, is becoming a limiting factor for the further miniaturization of packages due to the increase of current density and the shrinkage of solder joints.¹

Electromigration-related issues, such as current crowding, Joule heating, and mechanical behavior, have been widely studied since 1998.²⁻⁵ Chiang et al. have demonstrated that current crowding occurred in solder joints, and could enhance the local atomic flux along with the electron flow and expedite the migration damage.⁶ Current crowding was expected to accelerate void formation and propagation along the interface between the intermetallic compound (IMC) and the solder.⁷ Furthermore, the crowding region could produce local Joule heating, which also accelerates electromigration-induced failures.⁸

Recently, thermomigration has been regarded as an

additional reliability concern for solder joints. Thermomigration is triggered by thermal gradients across the solder joint. For a first-level solder interconnect, this type of thermal gradient is more evident due to Joule heating that accumulates at the chip side when the cross-sectional area of conductive lines on the chip is gradually decreased. The earliest report concerning the combined effect of thermomigration and electromigration has been given by Ye et al.⁹ More recently, the individual contribution of thermomigration to the failure of solder joints has been described by Huang et al.¹⁰ They found that Pb atoms moved to the lower temperature side and Sn to the higher temperature side in tin-lead composite solder joints. We have also observed a redistribution of Sn- and Pb-rich phases, during which Pb atoms moved to the lower temperature side in eutectic tin-lead solder joints at 150 °C.¹¹ In addition, we predicted a thermal gradient above 1000 °C/cm across these solder joints using numerical simulation.¹² The latest research by Hsiao and Chen has verified the existence of large thermal gradients across solder joints using a thermal imaging infrared technique, which provided further support to validate the numerical simulation results.¹³

The current carrying capability of solder/under bump metallization (UBM) and the heat dissipation of first-level solder interconnects should be incorporated on the basis of the electromigration and thermomigration limitations in design rules.¹⁴ Hence, the objectives of this study are to assess the electromigration and thermomigration behavior of eutectic tin-lead solder joints in terms

^{a)}Address all correspondence to this author.

e-mail: eeycchan@cityu.edu.hk

DOI: 10.1557/JMR.2008.0305

of Joule heating, microstructural evolution, and numerical simulation. The actual temperature of the solder joint was taken for accurate analysis.

II. EXPERIMENTAL

The samples used in this study were dummy test kits of flip chip packages from Practical Components (Los Alamitos, CA). The Al traces on the chip had a width of $105\ \mu\text{m}$ and a thickness of about $2\ \mu\text{m}$. The UBM layer was a thin film of Al/Ni/Cu, and the opening in the passivation layer for this UBM had a diameter of $102\ \mu\text{m}$. There were four rows of 12 solder bumps along each side of the chip. The bump diameter was about $190\ \mu\text{m}$. The test substrate was a FR4 board. The copper pad connected to the flip chip had a width of $152\ \mu\text{m}$ and a thickness of $35\ \mu\text{m}$. Moreover, to confine the dramatic growth of IMCs on the substrate side, the copper pad was electroplated with a thin nickel layer of about $3\ \mu\text{m}$. Both chip and substrate were daisy-chained for electrical continuity. The flip chip was attached to the substrate using a flip-chip bonder (SUSS, Garching, Germany). The bonded samples were then reflowed using a five-zone air convection oven. In the reflow temperature profile the peak was $220\ ^\circ\text{C}$, and the time above the liquidus temperature of the eutectic tin-lead solder was about 70 s.

Figure 1(a) is a typical bonded sample used for this study, and Fig. 1(b) gives a schematic diagram of flip chip solder joints in the marked region. Two pairs of solder joints (joints 5, 6, 7, and 8) were powered with currents ranging from 1.6 to 2.0 A above $100\ ^\circ\text{C}$, which was used to explore the electromigration effect. The average current density in the solder joint was calculated by dividing the applied current by the area of the passivation opening. Unpowered solder joints, especially the closest

ones (joints 4 and 9) to those stressed electrically, were investigated for the thermomigration study since no current was applied to them.

Both electromigration and thermomigration experiments were conducted in an oven, which was used to obtain a stable and uniform ambient temperature ranging from 20 to $150\ ^\circ\text{C}$. The real temperature in the Al trace under current stressing was deduced by a temperature coefficient of resistance (TCR) method. For the TCR calculations, a precision current source and a digital multimeter were used to obtain accurate resistance values of the interconnect structure. Four-point probe method was taken to remove the effect of test wires. Additionally, a thermal imaging infrared camera (FLIR, Portland, OR) with a sensitivity of $0.02\ ^\circ\text{C}$ and an accuracy of $\pm 1\ ^\circ\text{C}$, was used to monitor the temperature around the powered solder joints at a given temperature on a hot plate.

After the electromigration and thermomigration experiments, the samples were ground and polished towards the center of the solder joints. These cross sections were then examined using a scanning electron microscope (SEM) system.

III. RESULTS AND DISCUSSION

The electrical resistance of the aluminum traces, solder joints, and copper conductors under testing were estimated to be 201.2, 1.6, and $13.0\ \text{m}\Omega$, respectively. It is apparent that the Al trace is the primary heat source because of its larger resistance. Additionally, as the temperature coefficient of resistance of Al, eutectic solder, and Cu is of the same order of magnitude, the resistance increase of the Al trace makes the largest contribution to the resistance variation of this interconnect structure. Hence, the temperature in the Al trace can be deduced by

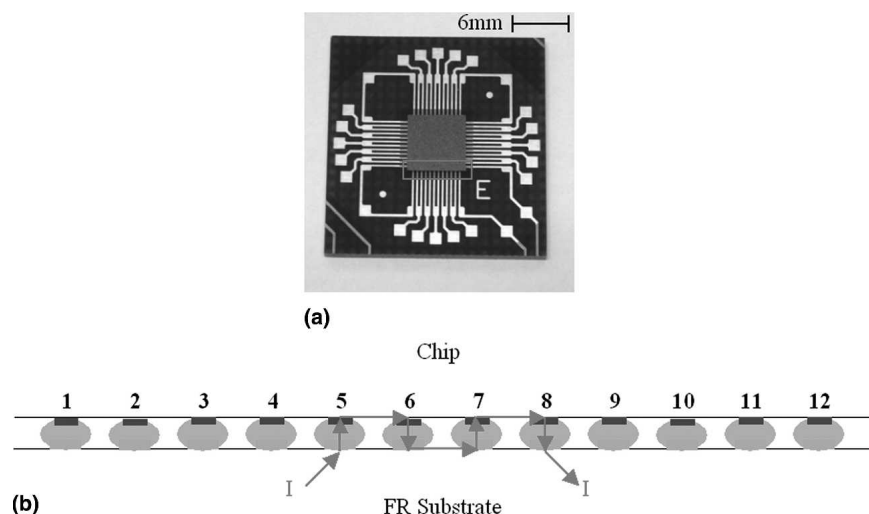


FIG. 1. (a) Flip chip module used in this study. (b) Schematic diagram of flip chip solder joints in the marked region (the arrow shows the positive current direction).

the TCR method. This method is an effective noncontact technique for the determination of temperature.

The calculation of TCR is typically expressed as

$$TCR = \left(\frac{R - R_0}{R_0} \right) \left(\frac{1}{T - T_0} \right) = \frac{\Delta R}{R_0 \Delta T} \quad (1)$$

where T_0 is the reference temperature (the ambient temperature under an experimental condition), T is the temperature in the Al trace, R_0 is the resistance of Al trace at T_0 , R is the resistance of Al trace at T , ΔR is the resistance variation, and ΔT is the temperature rise.

Figure 2 shows the TCR measurement results by the four-point probe method. The ratio of the resistance variation to the resistance at 20 °C (reference temperature) increased almost linearly over the temperature rise. The TCR equals the slope of $\Delta R/R_0$ versus ΔT . After curve fitting, the linear regression equation was found to be

$$\frac{\Delta R}{R_0} = -0.041 + 0.004 \Delta T \quad (2)$$

The TCR of the Al trace was estimated to be $0.004 \text{ } ^\circ\text{C}^{-1}$. By substituting the measured resistance into Eq. (1), the temperature in the Al trace can be obtained. Furthermore, since the Al trace is closely attached to the silicon chip with a large thermal conductivity, the temperature at the chip side can be monitored in situ in this way. Table I lists the calculated temperature of the chip with different currents and ambient temperatures. For the 1.6 A case, the temperature rise due to Joule heating varied from 3.8 to 13.9 °C depending on the reference temperature. In particular, for the 2.0 A case, at a reference temperature of 135 °C, the temperature in the chip was approximately 182.5 °C, close to the melting point of eutectic tin-lead solder.

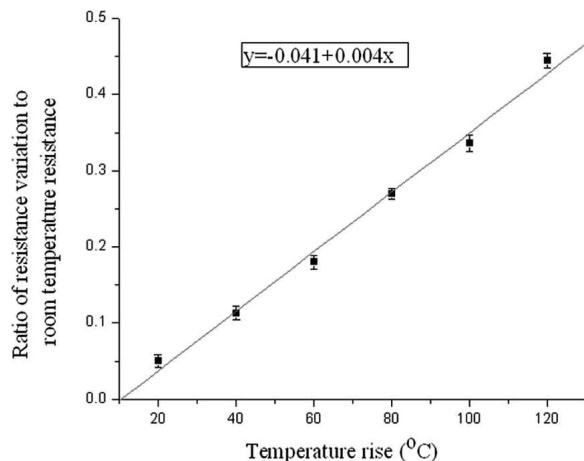


FIG. 2. Temperature coefficient of resistance measurement results of the interconnect structure (four-point probe method with a 100 mA test current).

TABLE I. Calculated temperatures, measured temperatures, and temperature deviations using two methods under the experimental conditions of currents and temperatures.

Ambient temperature T_0 (°C)	Current I (A)	Calculated chip temperature T_1 (°C)	Measured temperature around the chip T_2 (°C)	Deviation percentage of temperature $(T_1 - T_2)/T_2$ (%)
20	1.6	33.8	35.8	-5.6
20	1.8	51.8	49.9	3.8
20	2.0	61.4	59.2	3.7
100	1.6	113.9	110.0	3.5
100	1.8	133.2	118.0	12.9
100	2.0	158.1	147.3	7.3
135	1.6	138.8	142.0	-2.3
135	1.8	156.7	150.4	4.2
135	2.0	182.5	171.8	6.2

In addition, the local temperatures near the powered solder joints were detected using the infrared camera during the experiments. Table I also shows the measured temperatures near the powered solder joints. They agreed well with the calculated ones from the TCR method. The deviation percentage of temperature was insignificant, which was mostly less than 10%. More importantly, from these results, heat accumulation in the interconnect structure was found to be closely related to the current stressing.

A typical microstructure of a solder joint before the experiment (as-reflowed) is shown in Fig. 3. Fine scale Pb-rich phase particles (light regions) were uniformly dispersed in the Sn-rich matrix (dark regions). The UBM was found to be contacted well with the solder through an IMC layer at the interface on the chip side.

Figure 4 illustrates a typical electromigration phenomenon of tin-lead solder joints under a 1.6 A current (average current density $j = 2.0 \times 10^4 \text{ A/cm}^2$) after 100 h at 100 °C. Pb migration along with the electron flow was visible in the powered solder joints. Figure 5 shows the detailed microstructures of joints 7 and 8 at a higher magnification. Pb atoms had migrated toward the substrate side in joint 7. By contrast, Pb atoms had a tendency to migrate to the chip side in joint 8. Most Pb atoms migrated in the direction of electron flow, which agrees well with the findings of other researchers.^{2,15-18}

In addition, a tilting effect of the current during the electromigration process^{6,19,20} can be observed from Fig. 4. In joints 5 and 7, it is evident that the Pb-rich phase migrated towards and accumulated at the anode side corresponding to the entry direction of the electron flow. Moreover, as shown in Fig. 5(a), with downward electron flow, the mass flux was leaving than entering at the flux divergence plane, thus leading to the voids at the interface of the Cu-Sn IMC layer and the solder. Furthermore, under the electron wind force Ni atoms in the

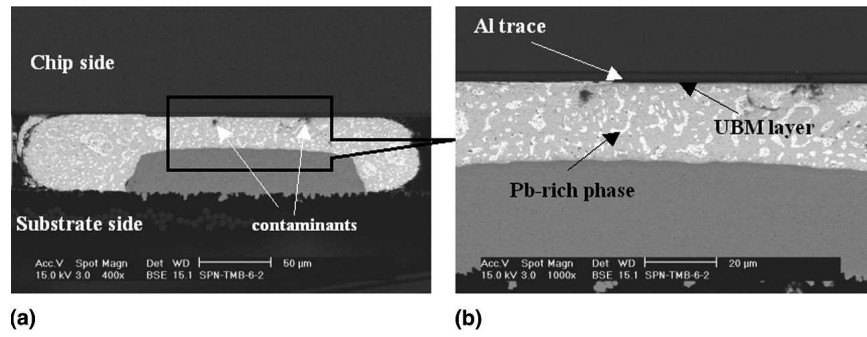


FIG. 3. (a) SEM micrograph of an original microstructure of solder joints (as-reflowed), (b) local magnified micrograph.

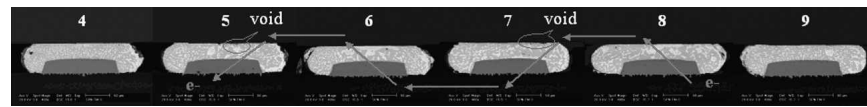


FIG. 4. SEM micrographs of a row of solder joints from joints 4 to 9, with solder joints from joints 5 to 8 under a current density of 2.0×10^4 A/cm² after 100 h at 100 °C (electromigration of Pb atoms in powered solder joints 5, 6, 7, and 8).

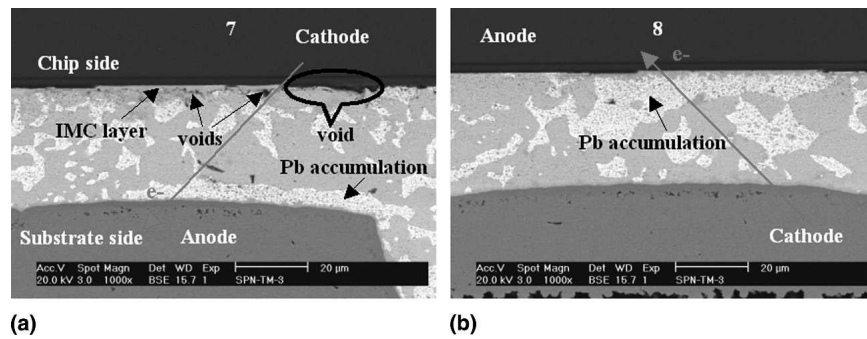


FIG. 5. (a) Local magnified SEM micrograph of powered solder joint 7 and (b) powered solder joint 8.

UBM (Al/Ni/Cu) were initiated to migrate downwards and formed the Cu–Ni–Sn compound. While the Ni was gradually consumed, the adhesion of the UBM with the solder began to degrade. Hence, more dramatic voids occurred at the interface between the metallization and the solder (the upper right corner). It is noticeable that these voids were primarily generated at the current crowding region because of concentrated flux divergence and more serious UBM consumption. It is expected that these voids would spread across the contact area with time extended and eventually cause failure.

To understand the characteristics of electromigration, thermal electrical finite element simulation was carried out. The parameters used in the simulation were taken from other researchers' work.^{8,21,22} The current density distribution of the solder interconnect with a 1.6 A current applied is shown in Fig. 6. According to the simulation result, the current density in most parts of the solder joint reached above 10^4 A/cm², which was sufficient to trigger atomic diffusion by the electromigration process. The existence of current crowding was also apparent. The current density at the entry location was predicted to be 7×10^5 A/cm², at least one order of magni-

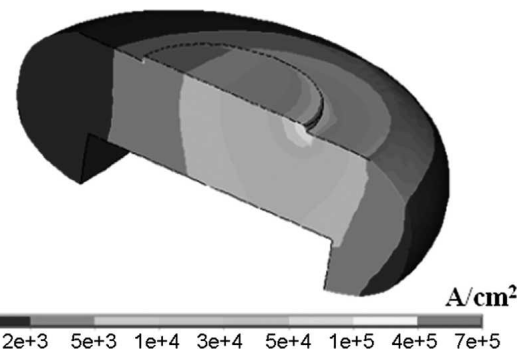


FIG. 6. Current density distribution of a solder joint stressed with a 1.6 A current.

tude larger than the average. This gives a reasonable explanation for the unique tilting effect that occurred in the solder joints. Near this current crowding region, atomic flux divergence also caused vacancy accumulation and hence voids, as shown in Fig. 5. In addition, the high current density may enhance local Joule heating and result in a temperature gradient across the solder joint, which may also contribute to atomic migration for the thermomigration.

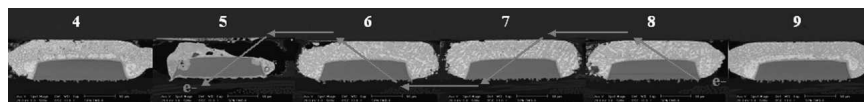


FIG. 7. SEM micrographs of a row of solder joints from joints 4 to 9, with solder joints from joints 5 to 8 under current stressing after 100 h at 135 °C (thermomigration of Pb atoms in unpowered solder joints 4 and 9).

Figure 7 illustrates a typical thermomigration phenomenon of tin-lead solder joints under a temperature gradient after 100 h at 135 °C. In this case, a 2.0 A current was applied to two pairs of solder joints (from joint 5 to joint 8) at 135 °C. Solder joint 5 was substantially damaged because of the Joule heating at the chip side. A dendrite structure of crystallization of liquid phase in other powered solder joints (joints 6 to 8) also suggests that they had been partially melted. These solder joints were subjected to a condition similar to reflow, during which the atoms within the solder joint had less tendency to be driven by electron flow. Therefore, no migration was observed in the powered solder joints. However, obvious thermomigration of Pb was detected in the neighboring unpowered solder joints (joints 4 and 9), as illustrated in Fig. 8. The Pb-rich phase was separated from the Sn-rich phase and accumulated at the bottom of solder joints. It is believed that Pb atoms migrated to the substrate side (the lower temperature side) under the temperature gradient across the unpowered solder joints since there was no current flow inside. This result basically agrees with those of thermomigration studies of tin-lead solder joints.^{10–13,23,24} The suggestion is that under a temperature gradient Sn atoms migrated relatively slowly and replenished the vacancies due to the departure of Pb atoms in a constant solder volume. Numerical simulation of the temperature distribution in our previous study also supported the existence of a thermal gradient.¹² Compared to that in the electromigration experiment, a larger chip temperature rise of 47.5 °C occurred in this case, as shown in Table I. This indicates that a larger thermal gradient was formed across the solder joints. Another important reason for thermomigration of Pb is the high temperature within the unpowered solder joints, which is

concerned with an accelerated diffusion at high temperature. According to Table I, in this thermomigration experiment, the chip temperature reached about 182.5 °C, near the melting point of eutectic tin-lead solder. In addition, recent studies have found that the solder microstructure was more uniform than the original after phase separation during the thermomigration.^{24–26} However, the phenomenon was not obvious in this case, in which the lamellar structure was not much finer and the morphology was similar to the phase separation that occurred in eutectic tin-lead solder due to electromigration, especially in solder joint 9. The condition under which thermomigration occurs is an interesting issue, and some attempt has been made in the present study to deal with this.^{12,24}

Figure 8(a) shows the void detected at the contact area between the UBM and the solder at the high-temperature side after thermomigration. It is reasonable that the driving force of gradient accelerated the atomic diffusion starting from the high-temperature region at this interface. However, the Cu–Ni–Sn IMC layer was not evident and the void propagation at the interface between the UBM and the solder was insignificant. This suggests that without the current crowding and the accompanying local heating, the atomic diffusion near the UBM region was relatively small. Moreover, unlike Sn or Cu electromigration, which has been well known to accelerate void formation during the electromigration,²⁷ the issue of migration of Sn and Cu atoms under the thermal gradient has been unclear and requires further investigation.

A stepwise cross-sectional analysis was conducted by gradually grinding the row of solder joints to the center of the passivation opening and examining with a SEM after each step. Figure 9 shows the cross sections of

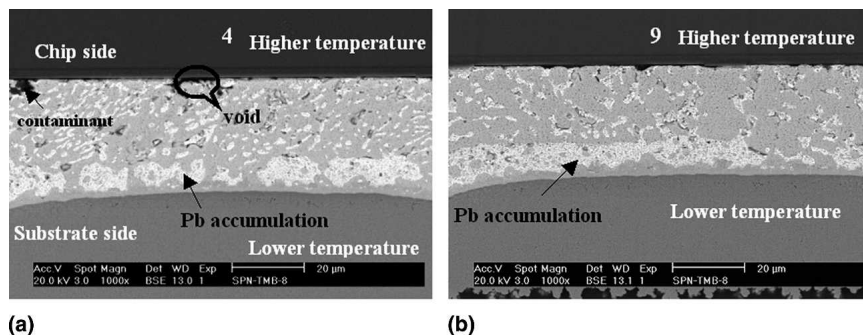


FIG. 8. Cross-sectional plane after the first polishing (outer solder). (a) Local magnified SEM micrograph of unpowered solder joint 4 and (b) unpowered solder joint 9.

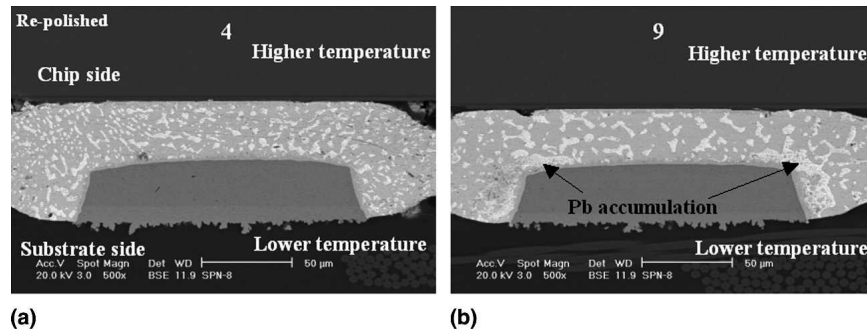


FIG. 9. Cross-sectional plane after repolishing 50 μm or so (inner solder). (a) SEM micrograph of unpowered solder joint 4 and (b) unpowered solder joint 9.

solder joints 4 and 9 after repolishing 50 μm or so. It is noted that the thermomigration of Pb was not as apparent as that in Fig. 8. In the solder joint 4, Pb-rich phases were uniformly distributed. Also, Pb accumulation in the solder joint 9 was slight and only Pb-rich phase at the periphery of the solder exhibited a thermomigration characteristic. This means that thermomigration at the inner solder was less significant than that in the outer solder (the surface layer). One can understand that temperature distribution inside the center of solder joint was uniform and hence a thermal gradient was not sufficient to initiate thermomigration. By contrast, it is easier to build up a large thermal gradient across the surface layer of solder joints where preferable heat dissipation was achieved, since the outer solder is close to the ambient. Therefore, different morphologies were observed at different cross-sectional planes even in the same solder joint. Similar phenomenon also occurred in other samples.

Additionally, the atomic flux due to electromigration (J_{em}) and thermomigration (J_{tm}) can be described as²⁸

$$J_{em} = N \frac{D}{kT} Z^* e \rho j \quad , \quad (3)$$

$$J_{tm} = N \frac{D}{kT} \frac{Q^*}{T} \left(-\frac{dT}{dx} \right) \quad , \quad (4)$$

where N is the atomic concentration, D is the diffusivity of the dominant diffusion species, Z^* is the effective charge number, ρ is the resistivity, j is the current density, Q^* is the heat of transport, and dT/dx is the temperature gradient.

Here, although it is likely that the thermomigration accompanied the electromigration process in the electromigration case, electromigration played the crucial role in driving the migration of Pb atoms since the temperature rise on the chip was not significant ($\Delta T = 13.9$ °C). Thus in the electromigration case the atomic flux of Pb due to thermomigration could be ignored in the total atomic flux. Hence, taking a Z^* of 10^3 a j of 2.0×10^4 A/cm², and the ρ as 1.46×10^{-7} Ω·m, the atomic flux of Pb in the powered solder joint was calculated to be

$\sim 3.4 \times 10^{14}$ atoms/cm² s for the electromigration experiment. On the other hand, in the thermomigration case, where no current was applied to the solder joints, the accelerated Pb diffusion was exclusively attributed to the driving force of thermomigration. Taking a Q^* of -25.3 kJ/mol,²⁴ an estimated dT/dx of 1000 °C/cm,¹² the atomic flux of Pb in the unpowered solder joint was determined to be 1.2×10^{14} atoms/cm² s, which exhibits the same order of magnitude as that in the electromigration case.

IV. CONCLUSIONS

This investigation established the importance of measuring the actual temperature of first-level solder interconnects to understand the electromigration and thermomigration behavior of solder joints. Both the temperature coefficient of resistance method and thermal infrared technique were applied to obtain the temperature at the chip side. It is indicated that the heat accumulation within solder interconnects is closely related to the current density.

This study made a comparison for the microstructural evolution which occurred in the electromigration and thermomigration cases. As the dominant diffusing species the migration of Pb atoms was detected during these two processes. For electromigration, the tilting effect of Pb migration was evident because of current crowding. Voids were primarily initiated at this current crowding region due to concentrated flux divergence, which demonstrated a more serious damage as compared with the thermomigration induced case. For thermomigration, the thermal gradient played a dominant role in the atomic migration. Different morphologies were detected at different cross-sectional planes in a solder joint, and thermomigration of Pb at the outer solder was more significant than that inside the solder center where the temperature distribution is relatively uniform. Both atomic flux of Pb due to electromigration and thermomigration was estimated to be on the order of 10^{14} atoms/cm² s.

Because it is a necessary trend for the application of

high current density packages, some measures, e.g., optimization of a thick UBM structure, should be taken to relieve the current crowding effect. New solder and UBM materials also need to be developed to endure high current density and large Joule heating. Meanwhile, the occurrence of thermomigration in solder necessitates further attention. Heat dissipation of solder interconnects should be enhanced in case of the establishment of a thermal gradient.

ACKNOWLEDGMENTS

The authors would like to acknowledge the financial support of CityU's Strategic Research Grant (Project No. 7002083). We also are grateful to the help from Prof. Y.Y. Hung at Department of MEEM, City University of Hong Kong for the infrared imaging test.

REFERENCES

1. International Technology Roadmap for Semiconductors: *Assembly and Packaging Section* (Semiconductor Industry Association, San Jose, CA, 2006), p. 2.
2. S. Brandenburg and S. Yeh: Electromigration studies of flip chip bump solder joints, in *Proceedings of the Surface Mount International Conference and Exhibition* (SMI, San Jose, CA, 1998), p. 337.
3. K.N. Tu: Recent advances on electromigration in very-large-scale-integration of interconnects. *J. Appl. Phys.* **94**, 5451 (2003).
4. G.A. Rinne: Issues in accelerated electromigration of solder bumps. *Microelectron. Relia.* **43**, 1975 (2003).
5. M.H. Lin and C. Basaran: Electromigration induced stress analysis using fully coupled mechanical-diffusion equations with non-linear material properties. *Comput. Mater. Sci.* **34**, 82 (2005).
6. K.N. Chiang, C.C. Lee, and K.M. Chen: Current crowding-induced electromigration in SnAg_{3.0}Cu_{0.5} microbumps. *Appl. Phys. Lett.* **88**, 072102 (2006).
7. L.Y. Zhang, S.Q. Ou, J. Huang, K.N. Tu, S. Gee, and N. Luu: Effect of current crowding on void propagation at the interface between intermetallic compound and solder in flip chip solder joints. *Appl. Phys. Lett.* **88**, 012106 (2006).
8. S.H. Chiu, T.L. Shao, C. Chen, D.J. Yao, and C.Y. Hsu: Infrared microscopy of hot spots induced by Joule heating in flip-chip SnAg solder joints under accelerated electromigration. *Appl. Phys. Lett.* **88**, 022110 (2006).
9. H. Ye, C. Basaran, and D.C. Hopkins: Thermomigration in Pb–Sn solder joints under joule heating during electric current stressing. *Appl. Phys. Lett.* **82**, 1045 (2003).
10. A.T. Huang, A.M. Gusak, K.N. Tu, and Y.S. Lai: Thermomigration in SnPb composite flip chip solder joints. *Appl. Phys. Lett.* **88**, 141911 (2006).
11. D. Yang, M.O. Alam, B.Y. Wu, and Y.C. Chan: Thermomigration in eutectic tin-lead flip chip solder joints, in *Proceedings of the 8th Electronics Packaging Technology Conference*. (IEEE, Singapore, 2006), p. 565.
12. D. Yang, B.Y. Wu, Y.C. Chan, and K.N. Tu: Microstructural evolution and atomic transport by thermomigration in eutectic tin-lead flip chip solder joints. *J. Appl. Phys.* **102**, 012716 (2007).
13. H.Y. Hsiao and C. Chen: Thermomigration in flip-chip SnPb solder joints under alternating current stressing. *Appl. Phys. Lett.* **90**, 152105 (2007).
14. L.N. Ramanathan, T.Y. Lee, J.W. Jang, S.H. Chae, and P.S. Ho: Current carrying capability of Sn_{0.7}Cu solder bumps in flip chip modules for high-power applications, in *Proceedings of the 57th Electronics Components and Technology Conference*. (IEEE, Reno, Nevada, 2007), p. 1456.
15. R. Agarwal, S.Q. Ou, and K.N. Tu: Electromigration and critical product in eutectic SnPb solder lines at 100 °C. *J. Appl. Phys.* **100**, 024909 (2006).
16. J.W. Nah, J.H. Kim, H.M. Lee, and K.W. Paik: Electromigration in flip chip solder bump of 97Pb₃Sn/37Pb₆₃Sn combination structure. *Acta Mater.* **52**, 129 (2004).
17. M.S. Yoon, S.B. Lee, O.H. Kim, Y.B. Park, and Y.C. Joo: Relationship between edge drift and atomic migration during electromigration of eutectic SnPb lines. *J. Appl. Phys.* **100**, 033715 (2006).
18. D. Gupta, K. Vieregge, and W. Gust: Interface diffusion in eutectic Pb–Sn solder. *Acta Mater.* **47**, 5 (1999).
19. J.W. Nah, K.W. Paik, J.O. Suh, and K.N. Tu: Mechanism of electromigration-induced failure in the 97Pb₃Sn and 37Pb₆₃Sn composite solder joints. *J. Appl. Phys.* **94**, 7560 (2003).
20. E.C.C. Yeh, W.J. Choi, and K.N. Tu: Current-crowding-induced electromigration failure in flip chip solder joints. *Appl. Phys. Lett.* **80**, 580 (2002).
21. M.G. Pecht, R. Agarwal, P. Mccluskey, T. Dishongh, S. Javadpour, and R. Mahajan: *Electronic Packaging: Materials and Their Properties* (CRC Press LLC, Boca Raton, FL, 1999), p. 25.
22. S.W. Liang, T.L. Shao, C. Chen, C.C. Yeh, and K.N. Tu: Relieving the current crowding effect in flip chip solder joints during current stressing. *J. Mater. Res.* **21**, 137 (2006).
23. Y.C. Chuang and C.Y. Liu: Thermomigration in eutectic SnPb alloy. *Appl. Phys. Lett.* **88**, 174105 (2006).
24. F.Y. Ouyang, K.N. Tu, Y.S. Lai, and A.M. Gusak: Effect of entropy production on microstructure change in eutectic SnPb flip chip solder joints by thermomigration. *Appl. Phys. Lett.* **89**, 221906 (2006).
25. A.T. Huang, K.N. Tu, and Y.S. Lai: Effect of the combination of electromigration and thermomigration on phase migration and partial melting in flip chip composite SnPb solder joints. *J. Appl. Phys.* **100**, 033512 (2006).
26. K.N. Tu: *Solder Joint Technology: Materials, Properties, and Reliability* (Springer Science + Business Media LLC, New York, 2007), p. 335.
27. W.J. Choi, E.C.C. Yeh, and K.N. Tu: Mean-time-to-failure study of flip chip solder joints on CuNi(V)Al thin-film under bump metallization. *J. Appl. Phys.* **94**, 5665 (2006).
28. P. Shewmon: *Diffusion in Solids* (TMS, Warrendale, PA, 1989), p. 223.